



# Main Examination Results of VVER-1000 Fuel After Its Irradiation in Power Reactors

*Yu. Bibilashvily<sup>1</sup>, K. Dubrovin<sup>2</sup>, I. Vasilchenko<sup>3</sup>, A. Yenin<sup>4</sup>, A. Kushmanov<sup>4</sup>, A. Smirnov<sup>5</sup>, V. Smirnov<sup>5</sup>*

<sup>1</sup> A.A.Bochvar Scientific Research Institute of Inorganic Materials (VNIINM), Moscow, Russian Federation

<sup>2</sup> Institute for Nuclear Reactors, Kurchatov Research Center, Moscow, Russian Federation

<sup>3</sup> OKB Hidropress, Podolsk, Russian Federation

<sup>4</sup> AO Novosibirskii Zavod Chimkoncentratov, Novosibirsk, Russian Federation

<sup>5</sup> Institute for Atomic Reactors, Dimitrovgrad, Russian Federation

## 1 Introduction

The main purpose of the VVER-1000 fuel examination was to study the efficiency of their operation at steady-state regimes during two or three cycles and to assess the potential for burnup and operation length extension. For this purpose the examination of the fuel assembly members was performed which enabled us to specify the properties of the materials and their influence on each other in power reactor operating conditions. On the basis of this examination the fuel assembly design was improved and the calculation codes were verified. Furthermore, the reasons and consequences of fuel failures were studied.

To date, nine fuel assemblies have been examined, one of which was - reference, two others - unsealed. All of them were discharged from the reactor without achieving the project burnup (Table 1).

## 2 Examination Program

All nine fuel assemblies were investigated according to one program including the following methods:

- visual inspection;
- measurement of overall dimensions;
- eddy-current test;
- gamma-scanning;
- X-ray and neutron radiography;

- analysis of gas pressure and composition inside fuel rods;
- ceramography/metallography;
- mass spectrometry;
- microanalysis and electron microscopy of fuel and fuel claddings.

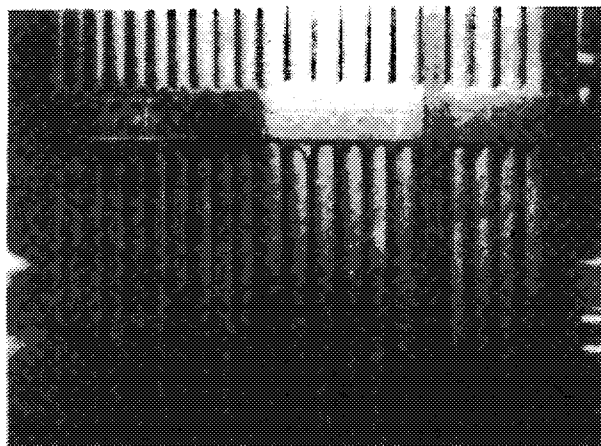
Using these methods the values of the main parameters were obtained characterizing the condition of fuel assembly and its structural members. The main of them are:

- change of fuel assembly and its members configuration;
- distribution of oxide film thickness along the fuel rod length;
- distribution of fuel cladding gap along the fuel rod length;
- state of fuel stack, welding, spacer grids, assembly, spring block and guides of absorber channels;
- distribution of fuel burnup, fission products and actinides along the height and radius of the fuel rods;
- distribution of material properties along fuel assembly volume, amount and character of hydrides in zirconium alloys;
- availability and character of defects.

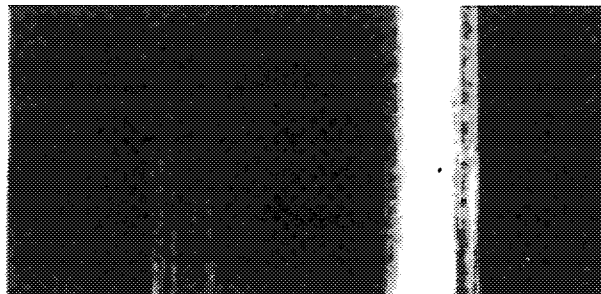
Additionally each fuel assembly was investigated by other methods determined by the specific research tasks, such as fuel refabrication with its further testing in the research reactors or in the in-cell stands.

**Table 1 List of the Examined VVER-1000 Fuel Assemblies**

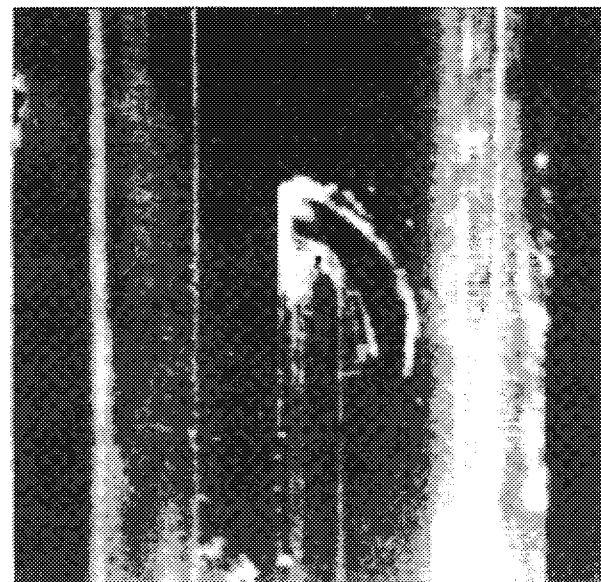
No.	FA	Reactor, NPP	Operation period	Duration eff. days	Average burnup	Initial fuel enrichment
1	0068	5-NVNPP	31.10.83 - 09.05.85	491	21.7	2.4; 3.0; 3.3
2	0007	5-NVNPP	12.09.82 - 09.05.85	825	32.6	3.3
3	0106	1-SUNPP	22.11.82 - 14.08.86	878.4	36.7	3.3
4	1114	5-NVNPP	25.06.84 - 25.06.87	923.1	44.7	3.6; 4.4
5	1565	2-Kal.NPP	05.11.85 - 02.07.88	838.7	34.7	3.3
6	1568	2-Kal.NPP	05.11.85 - 02.07.88	838.7	32.9	3.3
7	0623		10.10.88 - 17.06.89	236.8	19.5	3.6; 4.4
8	4108	5-NVNPP	05.07.86 - 11.07.90	881.4	46.2	3.6; 4.4
9	0619	1-Kal.NPP	10.10.88 - 23.11.91	859.5	42.4	3.6; 4.4



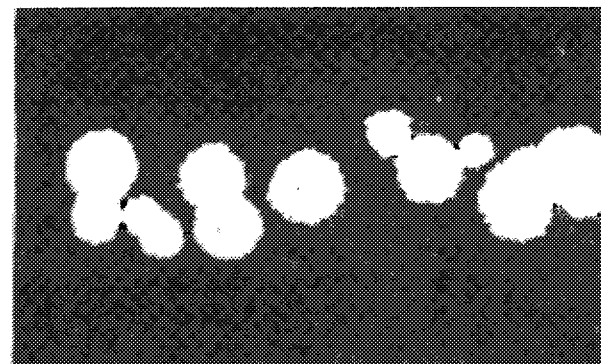
(a)



(b)



(c)



(d)

**Figure 1** Fuel assembly (a), fuel element (b), fuel cladding defect (c) and nodular corrosion (c).

### 3 Examination Results

#### 3.1 Visual Inspection

The visual inspection testified that there were no substantial changes in the fuel assembly design nor defects or configuration modifications of its structural members. The surface of cladding and wrappers was of dark color, typical for the autoclaved zirconium alloys (Fig. 1). The failed fuel rods were found to have defects caused the interaction of cladding with solid coolant particles. Moreover, some fuel cladding defects were observed which could be explained by spacer grid fretting-corrosion effect (Fig. 1). The nodular corrosion was found on the fuel rods of the South-Ukrainian assembly which was discharged after the disrapture of the main circulating pump and penetration of graphite into the coolant (Fig. 1). It could be caused by the specific microenvironment formed under the deposits of graphite compounds on the cladding.

#### 3.2 Dimensional Changes of Fuel Assembly and Its Fragments

In contrast to the VVER-440 the majority of VVER-1000 units use the wrapperless fuel assemblies. The bend of these fuel assemblies is of intricate shape and for the fuel assemblies represented in Table 1 achieves  $4.8 \text{ mm}$ . No evidence of the post-reactor elongation of the wrapperless fuel assemblies was noticed.

A substantial scattering of fuel rods elongation was observed even in one fuel assmeby (Fig. 2a). But an averaged elongation (Fig. 2b) had a linear correlation with fuel burnup.

The typical axial distribution of fuel rod diameter is given in Fig. 3. Taking into account the initial was observed of fuel pellet and inner cladding diameter it should be expected that in some cases the fuel-cladding gap will disappear even at burnups of  $35 \text{ MWd/kgU}$ . But the examination shows that on the average the decrease of fuel cladding diameter was observed at burnups up to  $50 \text{ MWd/kgU}$  (Fig. 4).

In the process of operation the channel guides of the safety and control rods take the shape of the fuel assembly. The change of length, outer or inner diameter was not detected. The measurement of spacer grid cells diameter revealed the increase of distinction between fuel rod diameter and that of grid cell being freed from the fuel rods (Fig. 4).

#### 3.3 Fuel Rod Cladding Condition

As a rule, after operation the inner surface of the VVER-fuel rod claddings was covered by dark uniform oxide film of  $4$  to  $8 \mu\text{m}$  thick which increases by  $1 - 2 \mu\text{m}$  in the upper part and practically does not depend on burnup (Fig. 5a). On the inner cladding surface the oxide film thickness modifies in the range from  $0$  to  $10 \mu\text{m}$  and it can be essentially changed along the cladding perimeter (Fig. 5b).

Sometimes claddings are found to have small quantities of lamellar form hydrides, the size of

which does not exceed  $50 \mu m$ . In this case the arrangement of the hydrides has random or tangential orientation (Fig. 6). The hydrogen content in claddings does not exceed  $(5 - 6) \cdot 10^{-3} \text{ mass\%}$ .

The mechanical properties of material claddings were practically the same for all the fuel assemblies that have been tested and are independent of the sample place and fuel burnup (Fig. 2). The yield strength at operating temperatures is no less than  $300 \text{ MPa}$ . As for the uniform and total elongation, they are respectfully no less than 4 and 15% at room temperature.

All types of VVER-1000 cladding failures which caused the premature discharge of fuel assemblies can be referred to the interaction of fuel rods with solid foreign particles. Some fuel assemblies were found to have essential cladding failures that did not result in fuel rod unsealing (Fig. 7).

### 3.4 State of Fuel Stack

The dimensions of fuel pellet central hole do not change in the burnup range covered (Fig. 8). The change of the grain size goes slowly (Fig. 9) and that points to the low (lower than  $1500^\circ\text{C}$ ) fuel temperature. The maximum dioxide uranium swelling does not exceed 4%. Fuel pellets are mainly fragmented by 3 to 5 parts preserving therewith its cylindrical shape. The fuel column length in some cases increases up to  $58 \text{ mm}$ .

The distribution of all radionuclide fission products (Fig. 10) points to the absence of the axial migration among them and confirms the low fuel temperature in the operation process. In the areas of spacer grids the decrease of radionuclide concentration is observed.

The radial distribution of fission products and actinides also points to the absence of their noticeable migration.

### 3.5 Pressure and Fuel Gas Composition

In the process of fuel burnup the fuel gas pressure slowly increases and for those fuel assemblies which have been tested did not exceed  $30 \text{ atm}$  (Fig. 11). The pressure increase was conditioned by the noble gas fission products release from fuel. The dependence of gas fission products release from the size of fuel grains has been found.

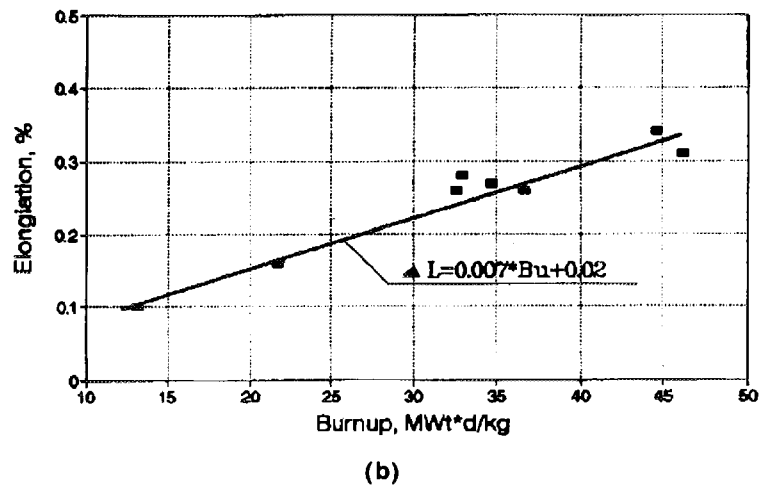
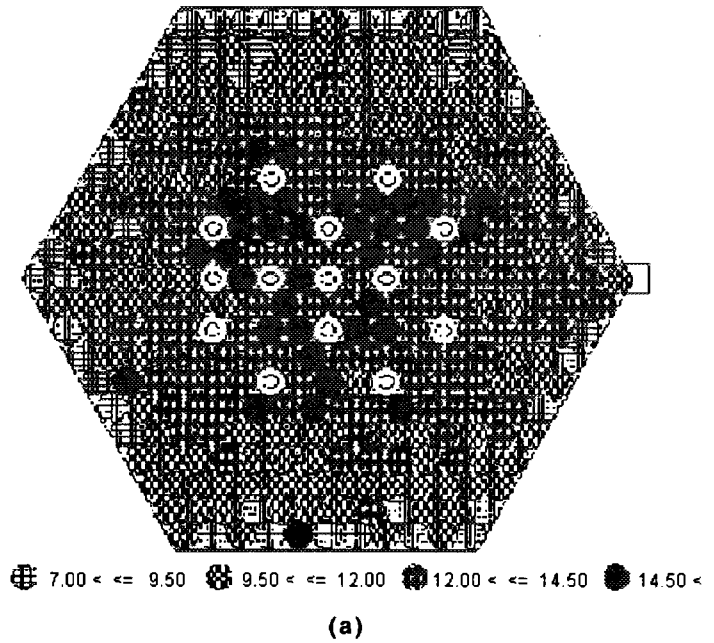


Figure 2 Elongation of fuel elements of VVER-1000:  
(a) elongation of fuel elements into fuel assembly;  
(b) dependence of fuel rod elongation on average fuel burnup

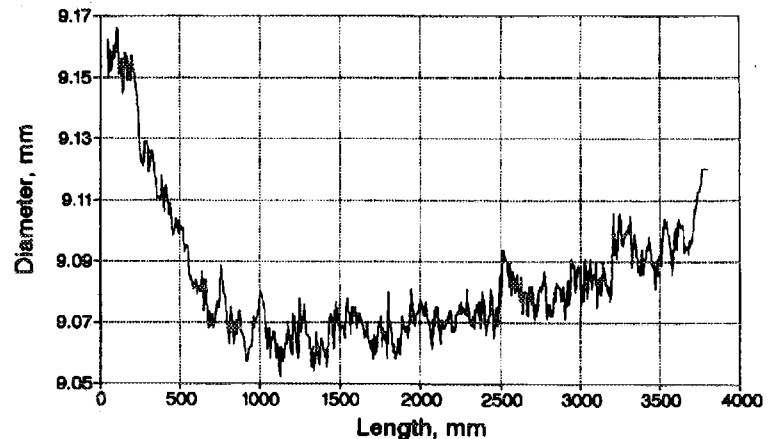


Figure 3 Distribution of fuel rod diameter size along length of the VVER-1000 fuel element

## 4 Conclusion

The examination results suggest that the VVER-1000 fuel spent at steady-state operating conditions up to 50 MWd/kgU of burnup is in satisfactory condition. The examination of all the types of the significant fuel cladding failures indicates that the reason lies in the interaction of cladding with coolant solid impurities. The nodular cladding corrosion of fuel assembly discharged from the South-

Ukrainian NPP is caused by the graphite compounds deposited on the fuel rod. Those depositions were a result of the circulating pump damage and beard an accidental, non-typical character. Some of the fuel rods were found to have a small cladding "fretting" of the spacer grid cell material.

The values of the majority of parameters determining the fuel efficiency allow an assumption that there is a potential for further extension of fuel burnup and operation length.

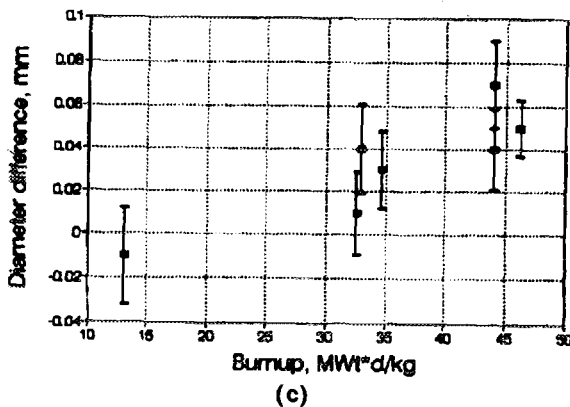
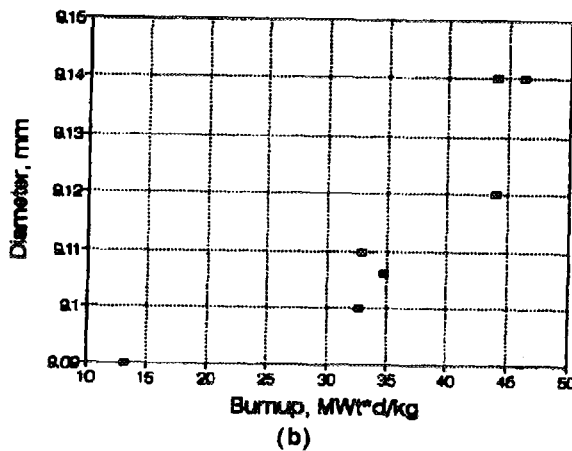
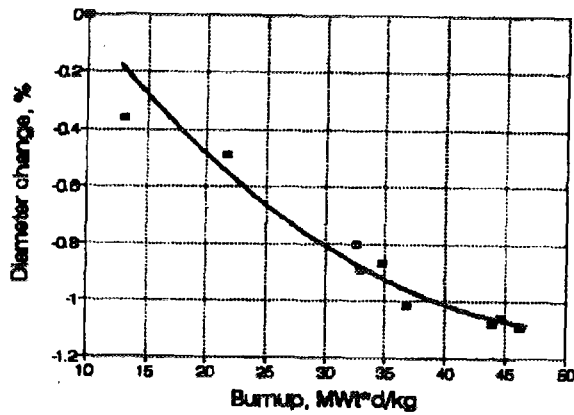
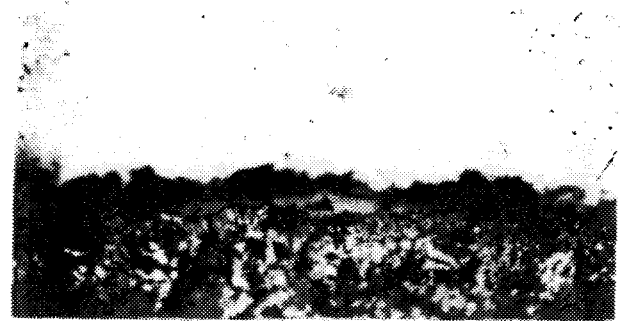


Figure 4 Dependence of fuel pin diameter change (a), spacers hole diameter (b) and diameter difference of spacer hole and fuel pin (c) on fuel burnup



(a)



(b)

Figure 5 The oxide film on the outer (a) and inner (b) surfaces

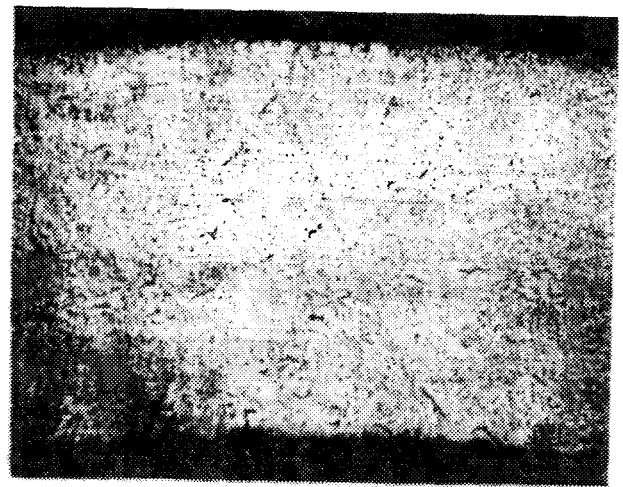
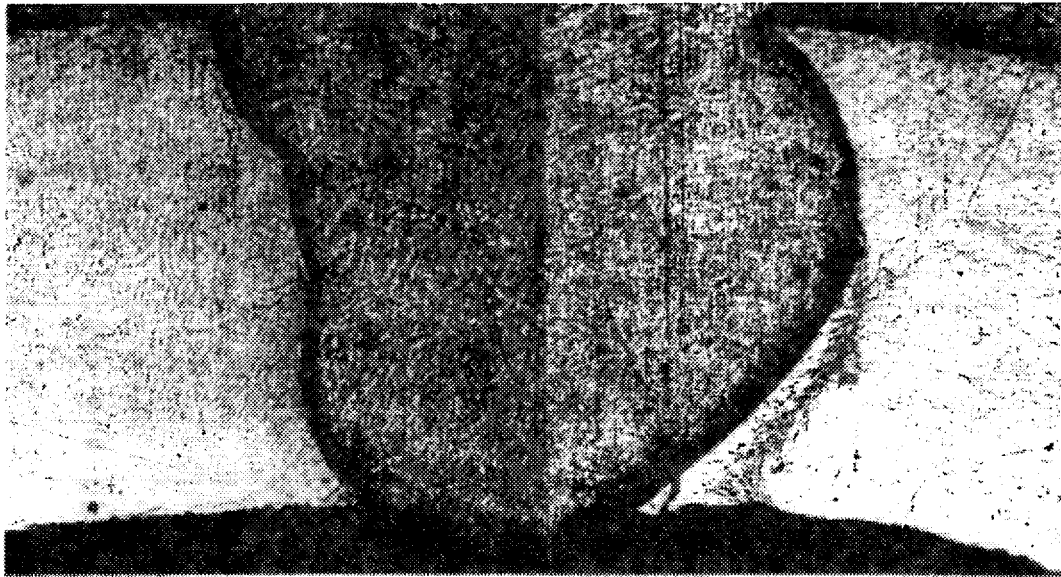
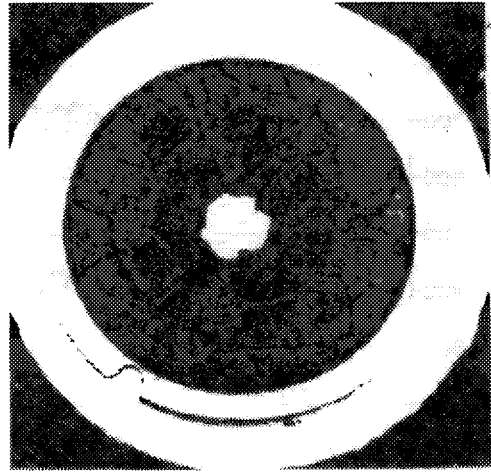
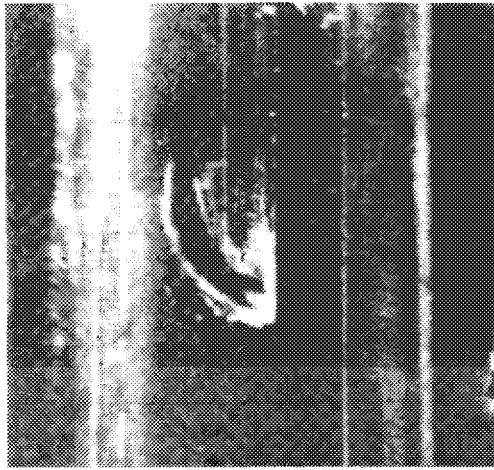
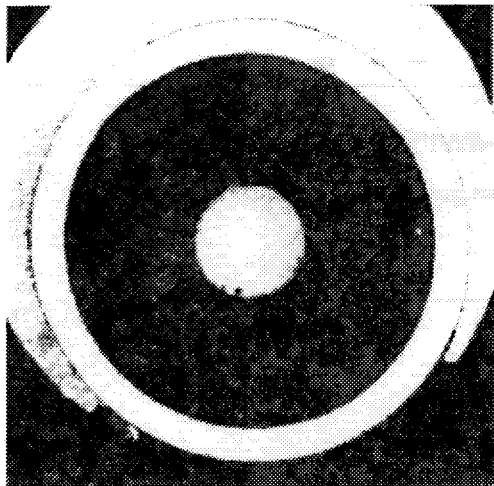


Figure 6 Characteristic structure of irradiated claddings



**Figure 7 Cladding defect**



**Figure 8 Fuel element macrostructure**

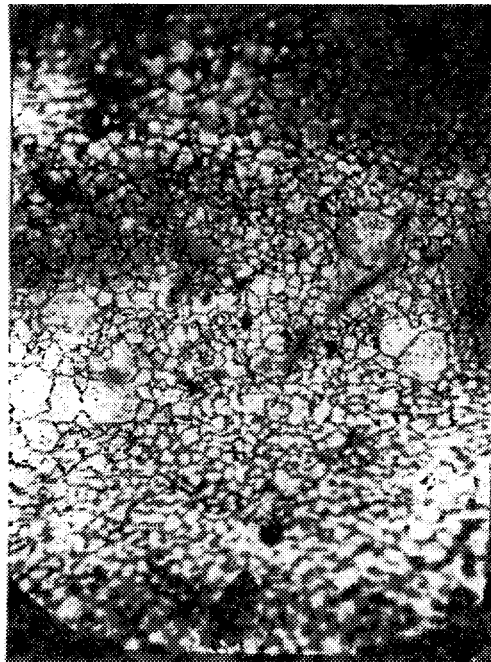


**Figure 9 Fuel microstructure**

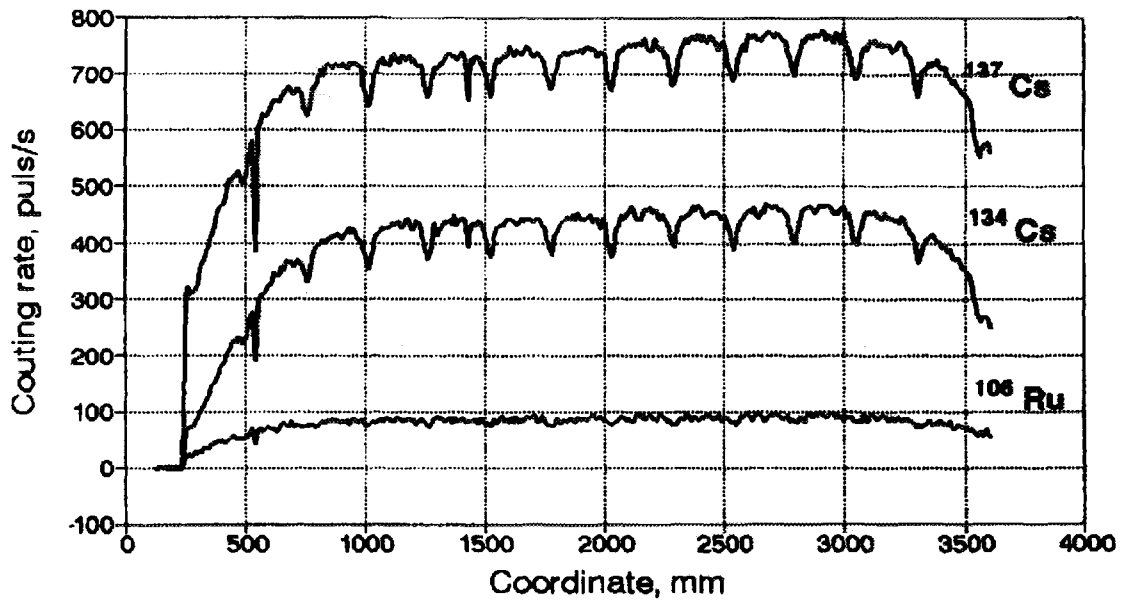


Figure 10 Distribution of fission products gamma activity along the fuel rod length

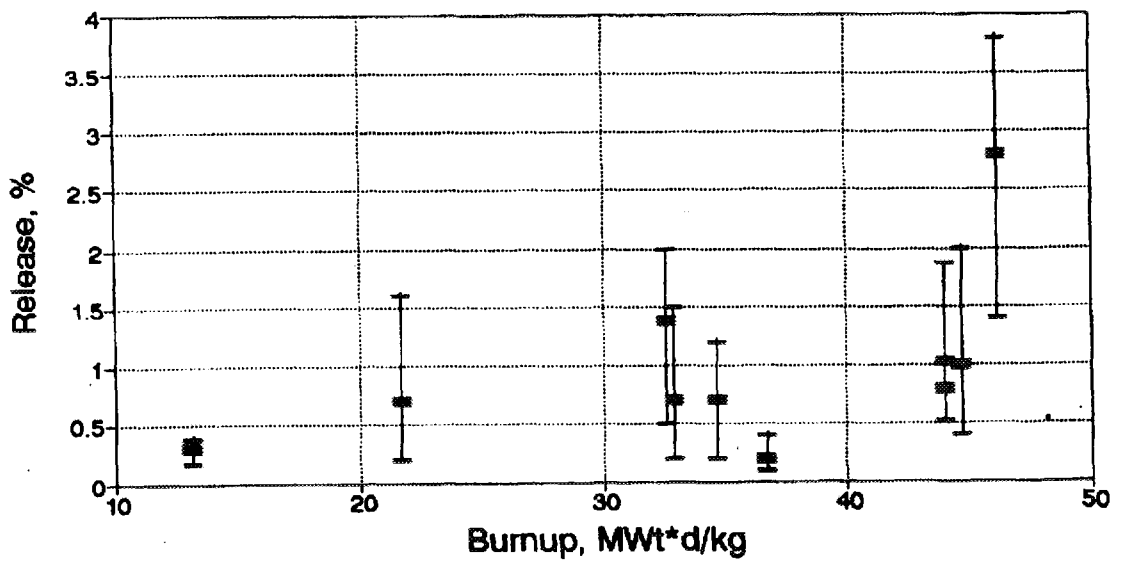


Figure 11 Dependence of fission gas release on burnup